

Lidar-based profiling of the tropospheric cloud-ice distribution to study the seeder-feeder mechanism and the role of Saharan dust as ice nuclei

Patric Seifert¹, Albert Ansmann¹, Ina Mattis¹, Dietrich Althausen¹, Matthias Tesche¹, Ulla Wandinger¹, Detlef Müller^{1,2}, and Carlos Pérez³

¹Leibniz Institute for Tropospheric Research, Permoserstr. 15, 04318 Leipzig, Germany. Email: seifert@tropos.de, albert@tropos.de, ina@tropos.de, dietrich@tropos.de, tesche@tropos.de, ulla@tropos.de, detlef@tropos.de

²Atmospheric Remote Sensing Laboratory, Gwangju Institute of Science and Technology, Republic of Korea. Email: detlef@gist.ac.kr

³Barcelona Supercomputing Center, Barcelona, Spain. Email: carlos.perez@bsc.es

1. INTRODUCTION

Heterogeneous ice formation in clouds at temperatures between -40°C and 0°C plays a major role in the production of precipitation in mid-tropospheric clouds and determines their radiative properties as well as their life time. However, the role of ice multiplication effects as ice particle splintering and cloud seeding, the so-called seeder-feeder mechanism (Rutledge and Hobbs 1983), to support the process of ice-formation in the troposphere remains unresolved. Also the initial formation of ice crystals at temperatures between 0°C and -40°C is still poorly understood (Cantrell and Heymsfield 2005). In this temperature range heterogeneous freezing of supercooled droplets must be initialized by aerosol particles acting as ice nuclei. In laboratory studies Saharan dust was found to be a favorable ice nuclei (Field et al. 2006) that is available in comparably high concentrations in the troposphere.

This study presents the investigation of heterogeneous freezing in natural mid-tropospheric clouds by means of polarization lidar measurements at a midlatitude site (51.3°N , 12.2°E). From a statistics based on observations of pure water and ice-containing clouds we investigated the influence of the seeder-feeder mechanism and of Saharan dust on the temperature-distribution of ice-containing clouds. Information about instruments and measurements used for the study are introduced in Sec. 2. Results are presented in Sec. 3. The impact of cloud-seeding and of Saharan dust on the freezing temperature of clouds is discussed in Sec. 4.

2. INSTRUMENTATION

The results presented in this abstract are based on measurements with polarization lidar. Here, a laser is utilized to emit pulses of co-polarized light. By detecting the returned light in the co- and cross-polarized direction, the depolarization ratio can be obtained which is a measure

of the non-sphericity of the atmospheric scatterer. Thus, spherical liquid water droplets cause no depolarization whereas non-spherical ice crystals cause significant depolarization to the scattered laser light. Hence, the depolarization ratio can be used to distinguish between liquid-phase clouds and clouds that contain ice crystals.

At Leipzig (51.3°N , 12.2°E), the vertically pointing three-wavelength Raman polarization lidar MARTHA (Multi-wavelength Atmospheric Raman lidar for Temperature, Humidity, and Aerosol profiling) (Mattis et al. 2004) has been employed for regular measurements since 1997. Besides other parameters it provides profiles of the depolarization ratio at 532 nm with a primary vertical resolution of 60 m and a temporal resolution of 30 s. 2344 hours of measurements performed with MARTHA between April 1997 and June 2008 built the basis for the DRIFT project (Dust-Related Ice Formation in the Troposphere). In the scope of DRIFT all measurements were screened for clouds which were then classified as described in Seifert et al. (2007). If a cloud layer was separated by more than 500 m in the vertical and 5 min in time from another cloud it was classified as a single cloud case. This ensures the classification of a cloud according to the meteorological conditions which led to its formation. Otherwise, long-lasting cirrostratus or altostratus cloud systems would impact a time-of-occurrence based statistic too strongly. Temperature information for each cloud case were obtained from regular radiosonde launches of the German meteorological service at Oppin, 30 km northwest of Leipzig. For times not covered by the radiosondes FNL/GDAS model data of the U.S. Weather Services National Center of Environmental Prediction (NCEP) was used (Information available at: <http://www.arl.noaa.gov/archives.php>).

Because MARTHA is pointed to the zenith, the signal received from ice-containing clouds can be significantly affected by specular reflection caused by horizontally oriented ice crystals. Specular reflection results in the mea-

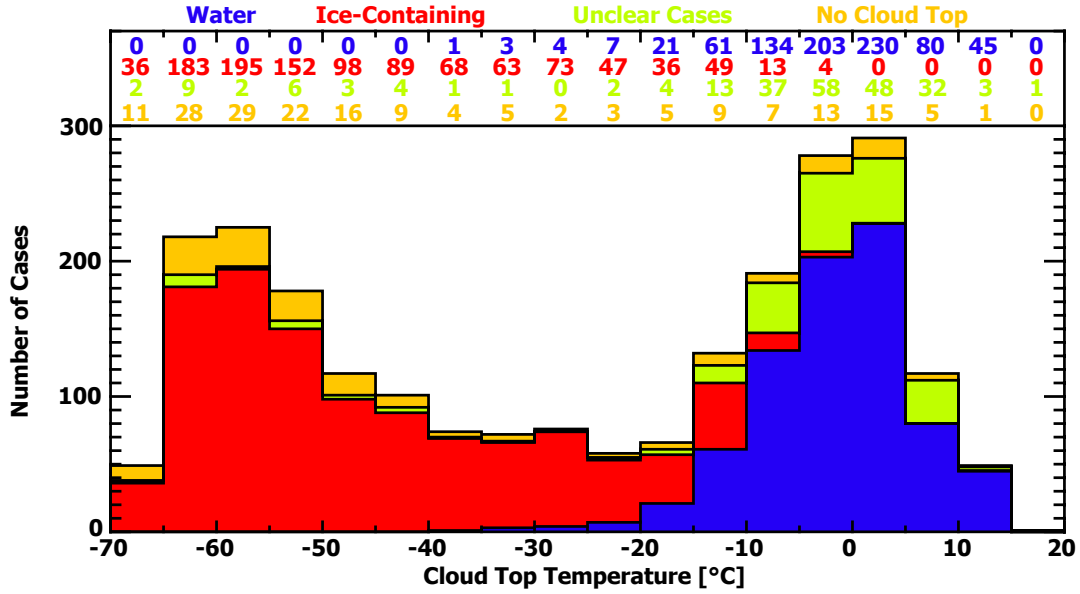


Figure 1: Numbers of well-defined cases of observed water clouds (blue) and ice-containing clouds (red), and unclear cases (undefined cloud phase), and cases with undefined cloud top for 5 K temperature intervals.

surement of depolarization ratios that are in the range of those produced by liquid water droplets. Thus, an unambiguous discrimination between ice and water layers within a cloud is not possible when a zenith-pointing lidar is applied. Therefore it was decided to categorize all observed clouds only into pure water clouds and ice-containing clouds which includes both, mixed-phase as well as pure ice clouds (Seifert et al. 2008).

In order to study the potential role of Saharan dust as ice nuclei for heterogeneous freezing (Field et al. 2006) information about columnar dust load at the grid point of Leipzig was obtained in 12-hourly intervals from the DREAM (Dust Regional Atmospheric Modeling System) model system (Pérez et al. 2006). This data was used to assign a measure of dust concentration to every observed cloud.

Table 1: Cloud observation statistics of the DRIFT dataset.

April 1997 – June 2008	Cases	Fraction
All Observed cloud layers	2319	
Well-defined cloud layers	1899	100%
Pure water clouds	789	42%
Ice-containing clouds	1110	58%
Clouds with $H_{\text{Top}} > 8$ km	774	41%
Clouds with $T_{\text{Top}} < -40$ °C	747	39%
Ice-containing clouds < 8 km	363	19%
Cloud phase undefined	236	
Cloud top undefined	184	

3. RESULTS

Table 1 gives an overview to all cloud observations. Out of 2319 observed cloud layers 1899 were well-defined, i.e. their phase and cloud top could be determined accurately. In 184 cases the cloud top could not be determined because of strong attenuation of the laser light. In 236 cases the cloud phase could not be determined. Reasons for that were technical problems with the depolarization channels or unclear depolarization signatures due to strong specular reflection or multiple scattering effects.

The distribution of the observed cloud cases with respect to cloud top temperature is shown in Fig. 1. The distribution is separated into contributions of water clouds (blue), ice-containing clouds (red), and undefined clouds for which either the cloud phase (orange) or the cloud top (green) could not be determined.

The fraction of ice-containing clouds with respect to all well-defined clouds of the DRIFT dataset is shown in Fig. 2 (asterisk). For comparison, results of four previous studies based on airborne in-situ measurements are shown (Korolev et al. 2003). All curves agree well. The slight shift of the DRIFT values to lower temperatures can be explained by the fact that the airborne in-situ observations are related to temperature at flight level whereas the DRIFT results are given as function of cloud top temperature which is usually the coldest point of a cloud.

4. DISCUSSION

In order to prevent an influence of low boundary layer clouds as well as of homogeneously nucleated cirrus clouds all subsequent investigations of the DRIFT data

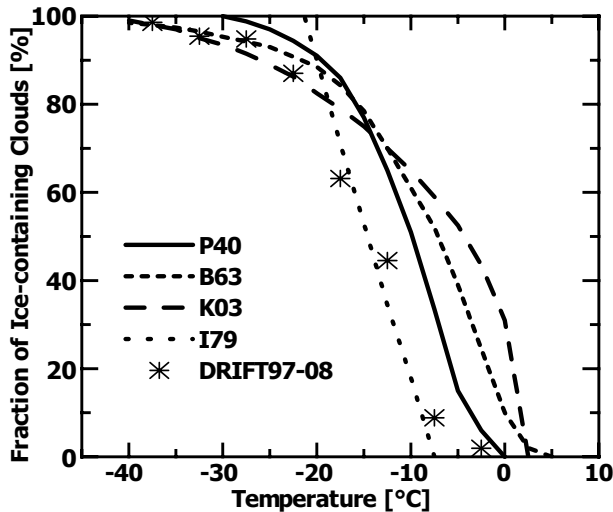


Figure 2: Comparison of the DRIFT observations with airborne in situ measurements at different mid-latitude sites (data are taken from Fig. 14 of Korolev et al. [2003]). Cloud observations of Pepler 1940 (P40), Borovikov et al. 1963 (B63), Isaac and Schemenauer 1979 (I79), and Korolev et al. [2003] are considered.

set were restricted to clouds that were detected between 3 and 8.5 km height.

4.1. Effect of the seeder–feeder mechanism

The vertical tropospheric distribution of cloud ice is expected to be in part determined by the seeder–feeder mechanism (Rutledge and Hobbs 1983). When several cloud layers occur, ice crystals falling out of the higher, colder cloud can act as ice nuclei in the lower, warmer cloud. This causes immediate glaciation of the seeded cloud that would be too warm for heterogeneous freezing to occur. The seeding effect therefore alters the radiative properties as well as the life time of the seeded cloud.

Whereas airborne observations can only probe the atmosphere at flight level, active remote sensing with lidar is capable of detecting multiple cloud layers. This allows the observation of the seeder–feeder mechanism. Ansmann et al. (2009) studied heterogeneous freezing in altocumulus clouds that were observed at Cape Verde (15° N, 23.5° W). A strong impact of cloud seeding on the distribution of ice-containing clouds in dependence of temperature was found. In a seeding–corrected data set all ice clouds were assigned to be water clouds if they were obviously seeded by crystals falling out of an ice cloud above. By applying this approach the fraction of ice-containing clouds of the Cape Verde dataset decreased to almost zero at temperatures above -20°C. The results of Ansmann et al. (2009) are shown as the thick solid and dashed curves in Fig. 3. The solid line represents the uncorrected data set whereas the dashed line shows the dis-

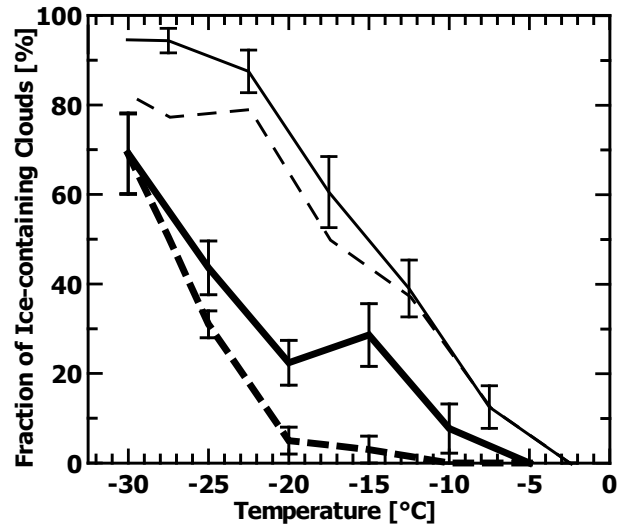


Figure 3: Comparison of the temperature dependence of the fraction of ice-containing clouds over the tropics (Cape Verde, [Ansmann et al., 2009]) and the European mid latitude station Leipzig. Thick and thin curves indicate Cape Verde observations and Leipzig observations (3–8.5 km only), respectively. The dashed curves show respective observations after screening the data sets for cloud seeding effects.

tribution of the ice-containing clouds of the data set that was corrected for the seeder–feeder effect. The same approach was applied to the DRIFT data set, shown as thin curves in Fig. 3. Here, an ice-containing cloud was assigned to be a water cloud when another ice-containing cloud was observed within 2 km above it. The difference between the uncorrected solid curve and the seeding–corrected dashed curve is smaller compared to the one of the Cape Verde data set. This is most probably because of the different meteorological conditions that lead to the formation of the clouds. Ansmann et al. (2009) observed predominantly thin layers of altocumulus clouds that are produced by weakly ascending air masses. An influence of frontal systems can be excluded in the region of the tropics. The clouds of the mid latitudinal DRIFT data set are to a high fraction influenced by meteorological processes that go along with the passage of frontal systems. Stronger updrafts, wind shear, and thus turbulence can be expected during the development of the midlatitude clouds. As Hobbs and Rangno (1985) pointed out, a broad drop–size spectrum is needed in order to trigger heterogeneous ice formation at temperatures $> -10^{\circ}\text{C}$. The higher fraction of ice–clouds and the smaller impact of cloud seeding at mid latitudinal sites compared to the tropics can therefore be best explained by the more turbulent conditions at mid latitudes which lead to the production of broader cloud–droplet spectra.

4.2. Role of Saharan dust as ice nuclei

In order to study the effect of Saharan dust on the heterogeneous-freezing temperature of clouds we used data of DREAM which, among other parameters, provides the columnal dust load at 00 and 12 UTC for the whole time period of the DRIFT dataset. By assigning a value of modeled columnal dust load to every observed cloud case we were able to separate clouds that were observed during dusty conditions from rather clean scenarios. The thresholds of dust load for the dust-influenced cases and for the presumably dust-free cases were set in such a way that a statistical significant number of cloud cases was available for both classes. Thus, a cloud case was categorized as presumably dust-free when the corresponding modeled dust load was $<0.03 \text{ gm}^{-2}$. At a columnal dust load $\geq 0.05 \text{ gm}^{-2}$ a cloud was categorized as a dust-influenced cloud. With these thresholds 189 dust-free cloud cases and 124 dust-influenced cloud cases were found. Figure 4 presents curves of the distribution of ice-containing clouds in dependence of temperature for the dust-free cases (circles) and the dust-influenced cases (stars). Vertical bars show the statistical error. Between temperatures of -20°C and 0°C the curves of the dust-free and dust-influenced clouds are clearly separated from each other. At all temperatures above -20°C the dust-influenced clouds show a higher fraction of ice-containing clouds compared to the dust-free clouds. Therefore, the presented findings corroborate the hypothesis that Saharan dust is an effective ice nuclei (Field et al. 2006). It should be noted that the curve of the presumably dust-free cases has a similar shape to the distribution of the only 90 cloud cases for which the columnal dust load was exactly 0.0 gm^{-2} .

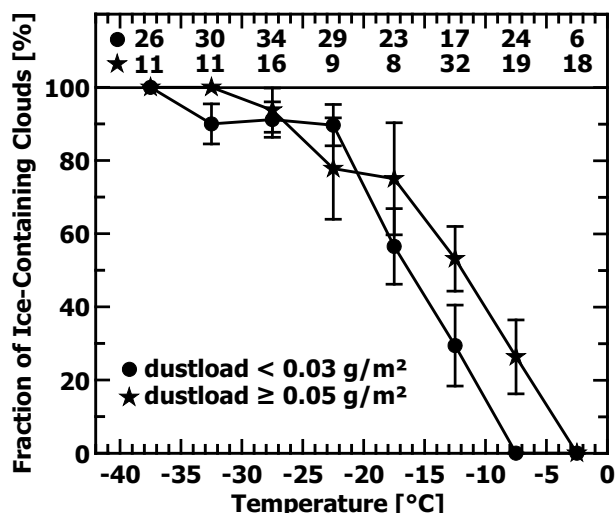


Figure 4: Fraction of ice-containing clouds for cases weakly affected by Saharan dust (circles) in comparison to cases strongly affected by Saharan dust (stars). Vertical bars show the standard error. Number of cases for each temperature interval are shown in the top area of the figure. Only clouds between 3–8.5 km were considered.

REFERENCES

- Ansmann, A., M. Tesche, P. Seifert, D. Althausen, R. Engelmann, J. Fruntke, U. Wandinger, I. Mattis, and D. Müller (2009). Evolution of the ice phase in tropical altocumulus: Samum lidar observations over Cape Verde. *Journal of Geophysical Research*, in press.
- Cantrell, W. and A. Heymsfield (2005, June). Production of ice in tropospheric clouds: A review. *Bulletin of the American Meteorological Society* 86, 795–807.
- Field, P. R., O. Möhler, P. Connolly, M. Krämer, R. Cotton, A. J. Heymsfield, H. Saathoff, and M. Schnaiter (2006, July). Some ice nucleation characteristics of Asian and Saharan desert dust. *Atmospheric Chemistry & Physics* 6, 2991–3006.
- Hobbs, P. V. and A. L. Rangno (1985, December). Ice particle concentrations in clouds. *Journal of Atmospheric Sciences* 42, 2523–2549.
- Korolev, A. V., G. A. Isaac, S. G. Cober, J. W. Strapp, and J. Hallett (2003, January). Microphysical characterization of mixed-phase clouds. *Quarterly Journal of the Royal Meteorological Society* 129, 39–65.
- Mattis, I., A. Ansmann, D. Müller, U. Wandinger, and D. Althausen (2004, July). Multiyear aerosol observations with dual-wavelength Raman lidar in the framework of EARLINET. *Journal of Geophysical Research (Atmospheres)* 109, 13203.
- Pérez, C., S. Nickovic, G. Pejanovic, J. M. Baldasano, and E. Özsoy (2006, August). Interactive dust-radiation modeling: A step to improve weather forecasts. *Journal of Geophysical Research (Atmospheres)* 111, 16206.
- Rutledge, S. A. and P. V. Hobbs (1983, May). The mesoscale and microscale structure and organization of clouds and precipitation in midlatitude cyclones. VIII: A model for the ‘Seeder-Feeder’ process in warm-frontal rainbands. *Journal of Atmospheric Sciences* 40, 1185–1206.
- Seifert, P., A. Ansmann, D. Müller, U. Wandinger, D. Althausen, A. J. Heymsfield, S. T. Massie, and C. Schmitt (2007). Cirrus optical properties observed with lidar, radiosonde, and satellite over the tropical Indian ocean during the aerosol-polluted northeast and clean maritime southwest monsoon. *J. Geophys. Res.* 112, D17205.
- Seifert, P., R. Engelmann, A. Ansmann, U. Wandinger, I. Mattis, D. Althausen, and J. Fruntke (2008). Characterization of specular reflections in mixed-phase and ice clouds based on scanning, polarization, and Raman lidar. In *Reviewed and revised papers presented at the 24th International Laser Radar Conference, 23–28 June 2008, Boulder, Colorado, USA*. Edited by the Organizing Committee of the 24th ILRC, ISBN 978-0-615-21489-4, pp.571–574.